Dynamics of a Grafted Chain in Contact with a Rubber Network: A Monte Carlo Study

J. M. Deutsch and Hyoungsoo Yoon*

Physics Board, University of California, Santa Cruz, Santa Cruz, California 95064

Received April 14, 1994; Revised Manuscript Received July 9, 1994®

ABSTRACT: The dynamics of a single chain tethered to an interface and in contact with a cross-linked network is examined numerically. When the network is put in contact with the tethered chain, the chain moves with dynamics that are highly constrained due to entanglements. When the surface is repulsive, the chain runs straight along the surface and then forms a plume in the network that starts at a distance of order $\sim N^{1/2}$ from the graft point. For short times, the chain length in the gel increases algebraically as a function of time, in most cases as $\sim t^{1/2}$. The plume configuration is highly metastable, and on a much longer time scale the point of entry into the network decreases to zero. This is similar to the relaxation of the arm of a star polymer in a cross-linked network. The above findings are in agreement with the analytical predictions of O'Connor and McLeish. The effects of a chemical disparity between the grafted chain, the network, and the substrate are investigated. Topological constraints are placed in the interface to determine their effects on the dynamics. Chains tethered at both ends are also studied and show a transition in behavior as a function of the thickness of the interface. Above a critical thickness the chain does not penetrate.

1. Introduction

1.1. Adhesion via Connectors. Polymer chains grafted to a surface or an interface have been the focus of extensive study during the past 15 years because of their practical importance. In particular, polymers grafted at the interface of two polymeric networks or solids often diffuse into the bulk, which will then increase the bonding of the two solids. This may be due to some type of chemical bonding between the grafted chains and the bulk polymers but can also be due to entanglements between them. Grafted polymers with such functions have been termed *connectors* for this reason.[1]

Since the junction is weaker than the bulk, the interface region usually fractures when an excessive stress is applied.[2] As the crack tip propagates along the interface, the chains either break or are pulled out, and this process is believed to contribute to the toughness of the interface.[3]

Although there have been numerous studies of the molecular mechanism of fracture for these systems, relatively little is known about the dynamics of the interface's formation. Understanding the dynamical aspects of this problem is important. As will be discussed below, the approach to equilibrium of these systems is often so slow that equilibrium conformations can never be achieved in the time scale of the experiments. Therefore the dynamics of these systems must be considered. Different models of chain pull-out, which make predictions about the toughness of an interface, make different assumptions about the dynamics. Since there are some discrepancies between different models,[1,2,4,5] it is important to have a better theoretical understanding of the dynamics as well as to perform further experiments. Another important application of the interface dynamics is in understanding the case of interface "healing". In the case where the toughness arises solely from entanglement effects, an interface can be healed even after a complete physical failure. To understand the recovery of the toughness upon recontact requires a detailed knowledge of the system's dynamics.

Recently, O'Connor and McLeish,[6] motivated by the experiment of Reichert and Brown,[7] investigated the relaxation of connector chains in an elastomer network attached to a glassy polymer. They considered the case where the chains are compatible with the elastomer but not with the surface of the interface. They found that there exist three stages in healing upon contact with the interface. First, the chain relaxes inside the interface. After this, the chain penetrates into the network. This is achieved in the Rouse time, and most of the toughness is recovered at this stage. On a much longer time scale, the penetration point moves logarithmically toward the point where the chain is anchored. The typical value of the total toughness gain by this *penetration-point-hopping* process was estimated to be 2.

Soon after the theoretical work of O'Connor and McLeish, Creton et al.[8] conducted a more detailed experiment, with some of the results apparently inconsistent with the current theories (see also Brown[9]). They carried out an experiment, which was originally devised by Johnson, Kendall, and Roberts,[10] on the interface between a cross-linked polyisoprene (PI) matrix and a polystyrene (PS) substrate grafted with PI chains. One interesting result of their work is that the dependence of toughness on molecular weight of tethered chains is not as strong as theories predict. It is hoped that a more complete understanding of the dynamics of the grafted chains will reconcile some of these inconsistencies.

1.2. Chain Pull-out Models. In this paper we consider the interface formed between a cross-linked polymer matrix and a rigid, nonreactive surface when connector chains with polymerization index N are end-tethered to the surface. The chains are assumed to be chemically compatible with the matrix unless specified otherwise and have a monomer size or *Kuhn length* of a.

The degree of the coverage is usually classified according to the surface density, σ, of the grafted chains. At low densities, $\sigma \ll 1/a^2N$, one has what is termed a "mushroom regime" since single chains that are repelled by a surface form a mushroom-like or plume-like shape in equilibrium.

In this paper we study this low-density regime where the interaction between different connector chains can be ignored, in which case we only need to consider the behavior of a single connector chain. The aim of the present work is to study the relaxation of a connector chain from a conformation lying on the surface to the equilibrium plume-like configuration. Experimentally relevant quan-

® Abstract published in *Advance ACS Abstracts*, August 15, 1994.

0024-9297/94/2227-5720$04.50/0

tities are obtained by averaging over the ensemble of these (noninteracting) chains.

What is the most relevant quantity one needs to measure to describe the toughness enhancement of the interface arising from the pull-out of a single connector chain? First we note that the chain pull-out process is viscous. Hence toughness enhancement due to the connectors should be a monotonically increasing function of the chain length inside the rubber. When the crack propagation speed is larger than a certain critical value, a simple theory[5] predicts that the toughness due to this energy loss when connector chain is pulled out is proportional to the square of the chain length inside the rubber. When this speed is small, Raphaël and de Gennes[1,11] formulated a theory which predicts that the toughness is linearly proportional to the chain length inside the rubber. As such, the chain length inside the rubber is expected to play an important role in describing the toughness recovery process and is therefore measured as a function of time in our simulation.

The rest of the paper is organized as follows. In the next section, we will give the precise definition of the problem under investigation and some important concepts will be introduced. After this the numerical model and the simulation algorithm will be given in detail.

Our simulation results will be discussed in the following sections. The initial expansion process after the contact of the two materials is studied in section 3. We study the dynamics of the chain with both ends tethered as well as that of the chain with only one end fixed. The double grafting is interesting not only because of its relevance to the initial relaxation of the singly grafted chain but also because this might have some interesting experimental applications. Section 4 considers the relaxation of the free end into the rubber. First, the theoretical model of O'Connor and McLeish will be discussed in section 4.1. The effects of chemical disparity between the chain and the matrix or between the chain and the substrate are also discussed here. Simulation results are presented in section 4.2. Section 5 studies a situation different from the ones above in that the dynamics of the grafted chain are constrained by entanglements even in the interface region. Rather different results are obtained due to this entanglement effect. Finally, we summarize our results and present some directions for further investigation in the last section.

2. Model and Simulation Procedures

2.1. Physical Model. Now we describe the overall picture of the chain penetration process. Initially the chain is assumed to be exposed to the air and hence to be spread out on the substrate with a thickness of order a, the monomer size. This is a result of the high surface tension in this situation. Therefore the initial conformation on the interface is assumed to be a two-dimensional random walk. Throughout this work we will ignore the interactions of the connector chain with itself.

In most of this work, the connector chain is assumed to be chemically compatible with the constituent polymers of the elastomer. We can quantify this by defining an affinity parameter between the chain and the wall, χ, which is the interaction energy per monomer between the chain and the wall relative to that between the chain and the gel, in units of k_BT. χ is assumed to be close to zero. In this case, the equilibrium conformation is plume-like, having dimensions of order of that of a free phantom chain. If there were no entanglements it should reach an equilibrium conformation in a Rouse time scale. However, the topological constraints imposed by the network prevent the chain from moving freely into the gel. Initially the chain is repelled from the surface and makes kink-like configurations or *excursions* that penetrate into the network. For the case of a chain with both ends tethered, this penetration by making excursions is the only mode of motion. Depending on the thickness of the slab and the chemical properties of the interface, the chain may penetrate into the network deep enough to contribute to the adhesion of the two materials. But for the singly tethered chain, the free end moves into the gel, at a point of order $N^{1/2}a$ from the tethered end, forming a plume. We will see that the plume pulls out much of the slack from the rest of the chain because this is entropically favored.

The plume size that initially forms depends strongly on the degree of entanglements in the interface. Even though we concern ourselves mostly with the low-coverage regime in which case the chains should move freely inside the interface, we discuss in section 5 the effects of entanglements in the interface. These should be present at higher densities and can be caused by interactions between grafted chains.

Let us suppose that a chain initially penetrates into the network at a distance $R \neq 0$ from the anchor site. Then we will see shortly that this conformation is in a metastable state with a very large relaxation time.[6] After the time scale associated with reaching this metastable plume state, the relaxation time depends exponentially on the penetrated length of the tethered chain. At times greater than this the chain relaxes by slowly shifting its entry point into the gel and eventually the total toughness is recovered.

2.2. Computer Simulation. The cross-linked network is modeled in this work by the so-called *cage model*. The cage model was first introduced by Doi[12] and Evans and Edwards[13-15] to investigate numerically the properties of the reptating polymers predicted by de Gennes.[16] The chain sits on a lattice with lattice constant a. The cross-linked points make another regular lattice (cage), which interpenetrates the former. The cage, which resembles a cubical "jungle-gym", imposes topological constraints on the motion of polymers. The distance between adjacent parallel bars is chosen to be the entanglement length d_e, which is usually assumed to be an integral multiple of the lattice constant a.

In this simulation, we only consider the case where the Kuhn length is the same as the entanglement length of the network, that is, $a = d_e$. In this case, if we consider both the cross-link points of the cage and the lattice sites the monomers can occupy, we obtain a lattice that is body centered cubic (bcc), which is bipartite. The cross-link points occupy one sublattice and the polymer moving around it occupies the other. The cage is restricted to $z \geq d_s$, where d_s is the thickness of the interface region. Due to the discreteness of the lattice, d_s is somewhat ambiguous and we use half-integer values for d_s because the cage lies halfway between lattice points. In most experiments in the low-coverage regime, the network is frequently in contact with the surface and thus $d_s = 1/2$ should correspond well to this situation. (Recall $d_e = a = 1$.) The case with general half-integer d_s's will be discussed briefly in the next section.

We tether one end of the N-mer chain at the origin and place the rest randomly on the surface, which is chosen to be the xy-plane with $z = 0$. (The other end is also tethered in section 3.) After this it moves into the gel network by dynamics that are described below. The chain is not allowed to penetrate into the wall ($z < 0$).

We choose an arbitrary bead other than the grafted end(s) and attempt to move it according to the following rules.

Move I: If it is the free end, it is moved to one of the six nearest neighbor points (on the same sublattice). Excluded volume effects are completely ignored in this work except for the presence of the hard wall.

Move II: If its two nearest neighbor beads along the backbone are on the same lattice point, then we move this middle point randomly to one of the six nearest neighbor points.

Move III: In most of the cases we study, there are no entanglements on the surface and so we must add one more move set. If the chosen point and its two nearest neighbor beads lie in the region $z < d_s$ and they form a right angle, we flip the middle bead through the diagonal made by the other two.

If the newly selected point (after the temporary move) does not violate the constraints imposed by the wall, we accept the move and update the conformation of the polymer. In the course of a simulation this procedure is repeated many times with beads that are chosen randomly.

In systems where there is an interaction between the chain and the wall, the case of nonvanishing χ, the acceptance probability is

$$\min(1, e^{-\Delta E/k_B T})$$

following the usual Metropolis algorithm. Here, ΔE is the energy change after the attempted move, which is $\pm\chi$ times $k_B T$ if the number of beads which are in contact with the wall changes by one.

We define a Monte Carlo step (MCS) as $N - 1$ such attempts for the singly grafted chain and as $N - 2$ for the doubly grafted one. One MCS corresponds to the monomeric relaxation time τ_1.

As mentioned in the previous section, the time dependence of the number of monomers in the penetrated part of the chain plays an important role in the toughness recovery process. So does the distance to the penetration point, R, in discussing the long time behavior. We measure these as well as other quantities such as the average height z_{av} and the radius of gyration in the vertical direction z_g. These are defined by the following equations:

$$z_{av} = \frac{1}{N}\sum_{i=1}^{N} z_i \tag{1}$$

$$z_g^2 = \frac{1}{N}\sum_{i=1}^{N} (z_i - z_{av})^2 \tag{2}$$

where z_i is the z-coordinate of the ith monomer.

In the following sections, we will analyze the dynamics of this system when χ is zero, negative (−ln(2)), and positive (ln(10)). To find out how far away these systems are from equilibrium, it is useful to have equilibrium statistics. These are easily obtained by using faster dynamics that do not have the topological constraints imposed by the network. To obtain these faster dynamics, we include the right angle flip (move III) everywhere along the chain. These moves can pass cage bars but give precisely the same equilibrium statistics. These dynamics have the relaxation time of the Rouse time ($\sim N^2$) and therefore give accurate results for equilibrium quantities. The equilibrium values of several quantities are tabulated for N = 20, 50, 100, and 200, and these will be used in the following sections. See Tables 1–3.

Table 1. Equilibrium Values of Various Quantities When There Is No Interaction between the Chain and the Wall, I.e., $\chi = 0$[a]

	length (N)			
	20	50	100	200
primitive chain length (L_{eq})	12.5	32.5	66.5	132.5
primitive length of the penetrated part (g)	11.5	31.5	65.0	131.5
radial distance to the entrance point (R)	1.1	1.1	1.1	1.1
no. of monomers on the trailing part (s)	3.8	3.6	3.5	3.5
height (z_{av})	1.5	3.0	4.4	7
radius of gyration (R_g)	1.0	2.8	4.1	5.7
vertical component of R_g (z_g)	1.0	1.6	2.2	3.3

[a] These were obtained using faster dynamics as explained in the text. Note that a is set to 1.

Table 2. Attractive Case: $\chi = -\ln(2)$[a]

	length (N)			
	20	50	100	200
primitive chain length (L_{eq})	6.0	14.5	30.5	66.5
primitive length of the penetrated part (g)	3.1	10.6	26	62
radial distance to the entrance point (R)	3.1	4.2	4.5	4.5
no. of monomers on the trailing part (s)	15.5	28.5	36.5	39
height (z_{av})	0.14	0.13	0.12	0.12
radius of gyration (R_g)	1.7	2.6	3.7	4.9
vertical component of R_g (z_g)	0.28	0.32	0.34	0.34

[a] While R_g is increasing as a function of N, there is no substantial increase in z_g, indicating the equilibrium conformation is pancake-like. Even though its thickness, z_{av}, is small, the penetration is appreciable in terms of g.

Table 3. Repulsive Case: $\chi = \ln(10)$[a]

	length (N)			
	20	50	100	200
primitive chain length (L_{eq})	13.5	33.5	67.0	133.5
primitive length of the penetrated part (g)	13.5	33.5	67.0	133.5
radial distance to the entrance point (R)	0.06	0.06	0.07	0.07
no. of monomers on the trailing part (s)	1.09	1.08	1.08	1.08
height (z_{av})	2.3	3.8	5.5	8.0
radius of gyration (R_g)	1.9	2.9	4.1	5.8
vertical component of R_g (z_g)	1.1	1.7	2.4	3.4

[a] The values obtained here are very close to those for $\chi = 0$ except R and s. The overall shape is vertically expanded slightly compared to the noninteracting case. In all three cases, $g + R = L_{eq}$.

Among those tabulated quantities the *primitive length* deserves some discussion. First, it is straightforward to see that the length of chain that has penetrated the network is an ill-defined quantity. It has an ambiguity for phantom chains when kinks are present at the penetration point. So, instead, we use the primitive path,[17] which is defined as the path of minimum length between the two end points that can be obtained by pulling all the slack from a chain without violating any topological constraints imposed by entanglements. The *primitive path length*, or *primitive length*, has been used in studying viscoelastic properties of polymers in a melt or a gel and is proportional to the total chain length in equilibrium. This yields an unambiguous definition of penetration length in our case: after finding the primitive path, we divide it into two parts at the penetration point. The number of beads in its penetrated part will be denoted by g. It will be extensively used in analyzing our simulations.

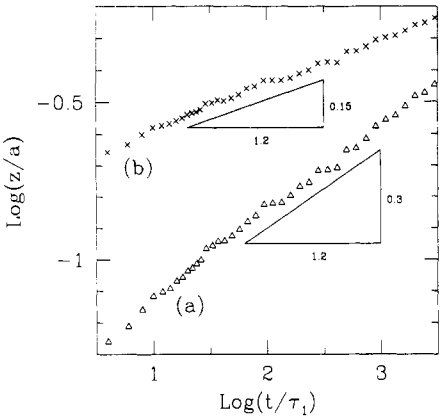

Figure 1. Log–log plot of the initial expansion of the grafted chain with $N = 200$. Both ends of the chain were fixed at the surface, and the data were collected from the middle portion of the chain. Here z denotes either (a) average height $\langle z_{av} \rangle$ or (b) vertical component of the radius of gyration $\langle z_g \rangle$. τ_1 is defined to be 1 MCS.

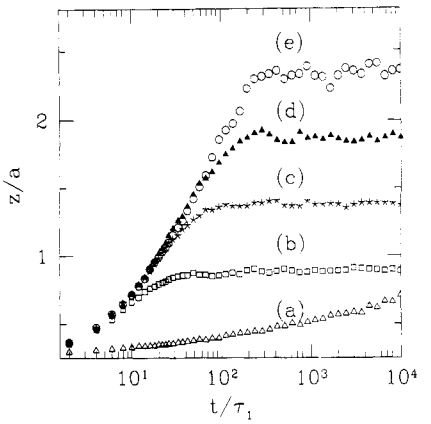

Figure 2. Penetration of kinks for various values of the slab thickness d_s. $N = 100$. (a) $d_s = 1/2$. (b) $d_s = 3/2$. (c) $d_s = 5/2$. (d) $d_s = 7/2$. (e) $d_s = 9/2$. The verticle axis is the average height $\langle z_a \rangle$ in units of a. Without penetration $\langle z_a \rangle$ is expected to be around $d_s/2$ in equilibrium. Except for the case $d_s = 1/2$, there is no substantial penetration.

3. Chains Tethered at Both Ends

3.1. Statics. We first study the case of a chain tethered at both ends. We create a chain as a two-dimensional random walk on the surface and fix both ends at these initial positions.

Even though there is no excluded volume interaction between the chain and the gel network, the topological constraint imposed by permanently attaching both ends of the chain to the substrate effectively generates a repulsive interaction between them. When the interface thickness d_s is bigger than a certain critical value, the penetration of the chain into the gel will be highly suppressed. This phenomenon is an example of *ground state dominance*[18] and in this case is due to a purely topological reason.[19] In other words, when the chain enters the network, its entropy is reduced due to the topology of the doubly grafted chain which restricts allowed conformations to only double back on themselves. If the interface is sufficiently thick, it maximizes its entropy by staying in the interface. However, if the interface slab is thin enough, it loses more entropy by staying in the interface than venturing into the network, and so it will be more favorable for the chain to penetrate into the network by making excursions. In such a case the height of the chain can grow beyond d_s depending on the amount of slack in the chain, which is the total chain length subtracted from the distance between the tethered ends. In fact, crossover behavior from an extended state to the collapsed one is expected when the thickness of the interface d_s is increased.

3.2. Dynamics. Upon attaching the rubber to the substrate, the thickness of the disk-like conformation of the connector increases to order d_s in a time scale of $\tau_1 (d_s/a)^4$.[18] That is, the height $\langle z_{av} \rangle$ averaged over the ensemble grows as $t^{1/4}$. This is shown in Figure 1 for $d_s = 1/2$.

Even though this was obtained for a sysetm in which both ends of the chain were fixed on the xy-plane, this initial penetration behavior is expected to be the same for the singly tethered case, because the free end becomes important on a time scale of $\tau_1 N^2$, as we will see in the next section. But to minimize boundary effects, the data shown here were collected only from the middle $N/2$ monomers.

This initial rapid growth stops when the average height reaches of order d_s. After this time scale the growth slows down. Figure 2 shows the slow penetration of kinks into the gel as a function of d_s. As stated earlier, penetration is achieved only for the case of sufficiently small d_s. As the figure suggests, when d_s is larger than 1/2, the saturation values of the *penetrated* height appear to be close to zero.

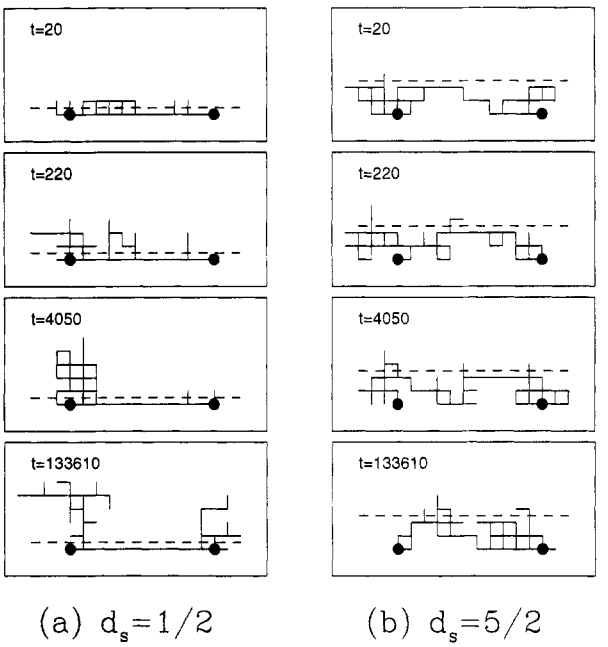

Figure 3. Relaxation of the doubly grafted chain in two dimensions. $N = 100$. (a) $d_s = 1/2$. (b) $d_s = 5/2$. The two circles represent the tethered points, and the dotted lines represent the thickness of the interface region.

Figure 3 shows that this is indeed the case. This picture was obtained from a two-dimensional system for the sake of clarity. There is a substantial penetration for the case $d_s = 1/2$, whereas for the case $d_s = 5/2$ there is very little penetration.

One interesting result is that the average radius of gyration in the z-direction, $\langle z_g \rangle$, has much weaker growth than the average height $\langle z_{av} \rangle$. As shown in Figure 1, the slope is 1/8 rather than 1/4. This shows that the chain as a whole translates away from the wall and penetrates the network at a much slower rate. The $t^{1/8}$ increase in $\langle z_g \rangle$ can be understood by noting that the loops in the network are lattice animals.[20] Lattice animals have a fractal dimension of 4 so that a loop in the network of m monomers has $\langle z_g \rangle \propto m^{1/4}$. The length of the loops increases by a diffusive process and therefore $m \propto t^{1/2}$. These two equations lead to the exponent of 1/8 found above.

4. Chains Tethered at One End

4.1. Theory. 4.1.1. Zero χ. In the previous section, it was shown that topological interactions limit the penetration of the doubly tethered chain. Topological constraints do not limit conformations accessible to the singly tethered case. In this case the network, in our numerical model, has no effect on equilibrium properties. In addition, when there is no attraction between the chain and the surface, we expect the chain will eventually reach the equilibrium plume-like shape mentioned earlier. As we now describe, the network affects the dynamics of this system in a drastic manner. The effects described below were recently worked out by O'Connor and McLeish.[6]

Once the chain end enters the gel, that portion of the chain in the gel is confined to a tube of diameter $\sim d_e$. The rest of the chain is constrained to the slab of thickness $\sim d_s$. Therefore we have two different relaxation modes, the snake-like motion of segments in the network and the two-dimensional Rouse motion for the rest. The segment of length $g(t)a$ will assume a plume-like conformation of size $g(t)^{1/2}a$ as it enters the gel. While this plume by definition starts at the surface, the center of the plume diffuses away from the wall because its size grows as more monomers enter the gel. Eventually the tension on the chain segment in the slab becomes big enough to counteract the pulling force of the free end, at which point the chain conformation will be "runner-like", in that it consists of a plume and a trailing part which connects the plume to the graft site. This is a metastable state as claimed earlier. Now we examine this process more quantitatively, giving a slightly simpler version of the argument of O'Connor and McLeish.[6]

Let us suppose the free end penetrates into the gel at a distance R from the origin. We will consider the statistical mechanics of this situation when the penetration point is held fixed. Then the free energy for the conformations, with s monomers in the slab, can be written as follows:

$$\frac{F}{k_B T} = \alpha\frac{R^2}{sa^2} + \beta\frac{sa^2}{d_s^2} \tag{3}$$

The first term is the elastic energy of the portion of the chain along the surface, and the second term represents the penalty due to its topological confinement in the slab.[18] The free energy is defined relative to that of a plume in true equilibrium, that is, when $R \sim d_s$. The numerical coefficients, α and β, are constants of order 1 and will be retained because their values can have important effects on the behavior of the system. These constants depend only on the geometrical properties of the system. For the case with nonzero χ, we have to add to eq 3 one more term which is proportional to s. This is neglected for the moment.

By minimizing this expression with respect to s, we get

$$s = \begin{cases} \dfrac{d_s R}{a^2}\left(\dfrac{\alpha}{\beta}\right)^{1/2} & \text{if } R < \dfrac{Na^2}{d_s}\left(\dfrac{\beta}{\alpha}\right)^{1/2} \\ N & \text{otherwise} \end{cases} \tag{4}$$

Since there is no metastable state in the latter case, the upper bound for R is $(Na^2/d_s)(\beta/\alpha)^{1/2}$. When the chain does penetrate, the segment in the slab is highly stretched in this local minimum because s is linearly proportional to R. This implies that most of the slack in the initial two-dimensional configuration of the chain must flow out of the slab and end up in the penetrated portion of the chain. This is a consequence of the unfavorable entropic conditions at the surface.

This entropic driving force will then lead to a rapid penetration of the chain by the diffusion of kinks, or defects, along the backbone of the chain. If we extend the concept of primitive path to include the slab[28] in addition to the tube, one can see that the primitive length is expected to increase in time. This is because the initial primitive length, $R \sim N^{1/2}$, is shorter than the value after long times when the chain is in its equilibrium state, in which case the primitive length, which is the sum of two parts one in the slab and one in the gel, is proportional to N. Hence the primitive length increases by diffusion of kinks. The growth of the primitive length is then proportional to $t^{1/2}$.

This process continues until the spring force of the segment in the slab of length $sa = Na - ga$ becomes comparable to the force due to confinement. The typical value of s at which the growth of $g(t)$ slows down is around $N^{1/2}$; i.e., $g \sim N$, as will be shown shortly. Hence $t^{1/2}$ growth persists until the time scale of $\tau_1 N^2$.

We now would like to compute the free energy barrier ΔF that these runner-like conformations must overcome to shift the penetration point closer to the point of tether. For these runner-like conformations, the free energy as a function of the entrance point R can be expressed as

$$\frac{F}{k_B T} = 2\frac{R}{d_s}(\alpha\beta)^{1/2} \qquad \left(R < \frac{Na^2}{d_s}\left(\frac{\beta}{\alpha}\right)^{1/2}\right) \tag{5}$$

The free energy barriers for these metastable states are the free energy differences between the runner states and the conformations when the whole chain is completely pulled out from the gel, that is, when $s = N$. Therefore

$$\frac{\Delta F}{k_B T} = \alpha\frac{R^2}{Na^2} + \beta\frac{Na^2}{d_s^2} - 2\frac{R}{d_s}(\alpha\beta)^{1/2} = \beta\left(\frac{a}{d_s}\right)^2\frac{g^2}{N} \tag{6}$$

The relaxation time of this metastable state is given by Kramer's formula

$$\tau_g = \tau_1 N^2 e^{\Delta F/k_B T} \tag{7}$$

$$= \tau_1 N^2 e^{\beta(a/d_s)^2(g^2/N)} \tag{8}$$

Compare this expression with the tube renewal time for a segment of length ga of the arm of a star polymer in a cross-linked network,[21,22] which is given by

$$\tau_{arm} = \tau_1 N^2 e^{\beta'(a/d_e)^2(g^2/N)} \tag{9}$$

where the constant β' comes from the confinement of the chain in a tube of diameter d_e and will presumably be larger than β.[17]

Therefore we see that the plume formed at R can tunnel into nearby local minima in a time scale of τ_g, thereby reducing the free energy given by eq 5. This penetration process is finally completed when R reaches of order d_s.

4.1.2. Nonzero χ. In the previous section it was assumed that the connector chain was chemically identical to the constituent polymers of the elastomer. Now we discuss the more general situation of nonzero χ.

First, we study the attractive case, $\chi < 0$. Attractive molecular forces, such as van der Waals forces, between the grafted chains and the substrate will give rise to a

negative χ as will the chemical incompatibility between the chains and the network. The fact that the tethered chains have to swell the cross-linked network is another reason for χ to become negative. Because the surface represents an infinite potential barrier, small negative χ is not enough to localize the chain to the surface. There is a critical value of attraction $\chi^* < 0$ giving two distinct types of equilibrium behavior. For $\chi > \chi^*$ the chain behaves much the same way as described in the previous section when $\chi = 0$. For $\chi < \chi^*$ the chain will spread out on the surface in a pancake-like conformation, giving rise to a finite chain thickness z_{av} independent of chain length. This is another situation characterized by ground state dominance.

Table 2 is obtained for $\chi = -\ln(2)$. The average height of the chain is about a quarter of $d_s = a$ regardless of the size of the chain, N, indicating this $|\chi|$ is much bigger than $|\chi^*|$. But even for such a strongly adsorbed case, the penetration is appreciable as shown in Table 2, and we expect strongly adsorbed grafted chains to make a significant contribution to the toughness of the interface.

Finally we mention the case with positive χ. The case with $\chi = 0$ is already a strongly repulsive situation, since grafted chains are excluded from the wall because of the excluded volume constraint. In fact the limit $\chi \to \infty$ is equivalent to taking $\chi = 0$ and making the wall thicker. Therefore no qualitatively different results are expected in the case of positive χ. However, the simulation results deviate from this expectation due to a problem with Monte Carlo dynamics. This will be discussed in the next section.

4.2. Simulation Results. 4.2.1. Zero χ. First we note that for the bcc lattice cage model with $a = d_e$ analytic solutions can be obtained exactly for many equilibrium properties.[23,24] Among others, the average primitive length in equilibrium, L_{eq}, can be easily calculated using the fact that the primitive path is a nonreversible random walk. L_{eq} is given by

$$L_{eq} = \frac{q-2}{q}N \tag{10}$$

where q is the coordination number of the sublattice where the polymers reside, which is 6 in our case, and so

$$L_{eq} = \frac{2}{3}N$$

Simulation results given in Table 1 are remarkably close to the above formula.

Now we discuss the penetration of the chain into the gel. As was mentioned earlier, this process can be understood as the diffusion of kinks out of the surface region and into the plume region and is driven by the entropy loss in the vicinity of the surface. The regime of rapid penetration of the chain is shown in Figure 4 for $N = 50$. Almost all the segments are inside the gel by the time $t \sim 10^5\tau_1$.

Figure 5 demonstrates scaling behavior for chains of different lengths, in this case $N = 20$, 50, 100, and 200. The vertical axis is scaled by the number of monomers, N, and the time axis by $\tau_1 N^2$, that is

$$g(t) = N\tilde{g}\left(\frac{t}{\tau_1 N^2}\right)$$

Therefore the relaxation time $\propto N^2$ as with Rouse relaxation. The log–log plot for $N = 100$ is shown in the inset and fits well to a straight line with slope 1/2.

These data were obtained, as stated earlier, with random walk initial conformations, which probably differ somewhat from experimental conditions. However, we have found that the result of $t^{1/2}$ growth is not very sensitive to the initial conditions, because all but the typical value of $R \sim N^{1/2}a$ are suppressed in the initial penetration step. If the chain is initially stretched, it contracts first to a Gaussian shape to reduce the tension before the chain enters the network. As an extreme example demonstrating this point, we prepared "samples" in which the grafted chains were initially stretched completely, say along the x-axis. The behavior for $g(t)$ was very similar to the case with random walk initial conditions. But, as we can see in Figure 6, the initial penetration was clearly suppressed compared to the previous case. The inset compares the approaches of the penetration points to the origin. In contrast, the samples with the chain initially bunched up near the origin have a slight advantage. This head start is reflected in Figure 6 as a small left shift of the curve.

In a much longer time scale after the chain reaches the first metastable state, the relaxation is similar to that of a star polymer in a network. In our case, the penetration point relaxes slowly toward the origin by retracting the arm into the slab.

Since the initial value of R is typically $N^{1/2}a$, the increase of g at this last stage is of order $(d_s/a)N^{1/2}$, which is negligible unless $d_s \gg a$. The system gains almost all its toughness in a time $t \sim \tau_1 N^2$. Note also that the increase of toughness after this time scale proceeds very slowly because in situations with even moderate chain length,

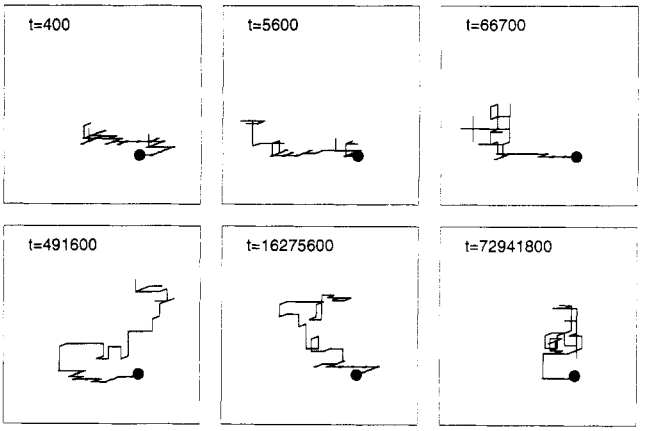

Figure 4. Penetration of the free end for $N = 50$. $d_s = 1/2$. The tethered point is represented by a filled circle. When $t = 66700$ ($>\tau_1 N^2$), we see the segment in the slab is highly stretched. This is the runner-like conformation mentioned in the text. The entry point into the rubber gets shortened as time goes on.

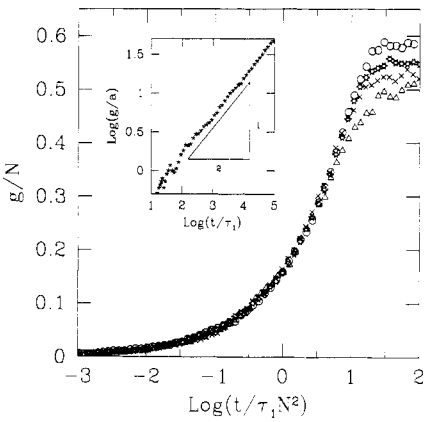

Figure 5. Scaling plot for $N = 20$, 50, 100, and 200. The verticle axis is the primitive length of the penetrated part, g, scaled by N, and the horizontal axis is the logarithm of t scaled by $\tau_1 N^2$. The inset is the log–log plot for $N = 200$. The exponent is 0.5.

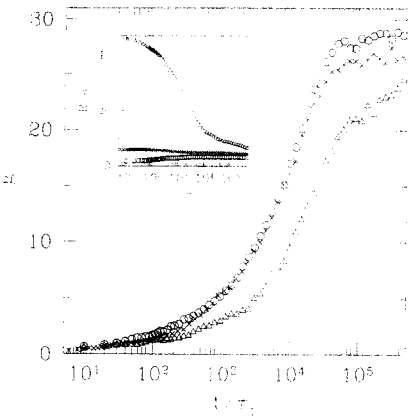

Figure 6. Comparison of the cases with different initial conformations. $N = 50$. $d_s = 1/2$. The primitive length of the penetrated part, g, is shown for the compact (circle), random walk (cross), and stretched (triangle) initial conformations. The inset shows the relaxation of the penetration point toward the origin. After the Rouse time the relaxation is logarithmic for all three cases.

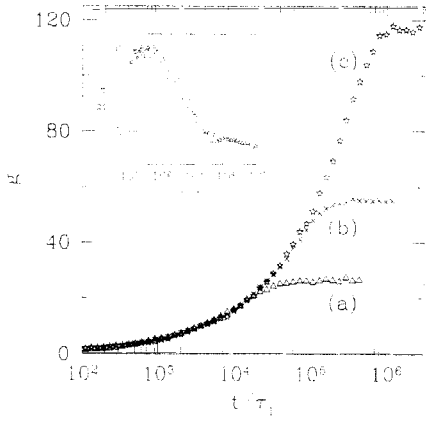

Figure 7. Increase of the penetration length as a function of time. After the initial power-law growth, it crosses over to logarithmic behavior. (a) $N = 50$. (b) $N = 100$. (c) $N = 200$. The crossover behavior is also apparent for the penetration point relaxation shown in the inset for $N = 50$.

the characteristic time, $\tau_1 N^2 e^{\beta(a/d_s)^2 N}$ is very large compared to $\tau_1 N^2$. Figure 7 shows that $g(t)$ increases until it reaches a saturation value $\sim N$. The inset is for $N = 50$ and shows the penetration point approaching the origin in an exponential time scale. Systems with N larger than 50 did not get to the last stage in a reasonable simulation time.

4.2.2. Nonzero χ. First we examine the attractive case numerically. Figure 8 shows the case $\chi = -\ln(2)$ for different chain lengths. They scale as

$$g(t) = N\tilde{g}\left(\frac{t}{\tau_1 N^{5/2}}\right)$$

for short times, $t < \tau_1 N^{5/2}$, indicating the growth is initially $t^{2/5}$. The log–log plot in the inset shows that the exponent is indeed close to 0.4. The reason why the exponent for the attractive case is 0.4 is unknown. It is also apparent that the toughness increases rather quickly with time, again indicating that this situation should lead to an enhancement of toughness in an experimentally accessible time scale. This penetration process for the attractive case is shown in Figure 9 for the two-dimensional case.

When the substrate is another rubber-like material instead of an impenetrable surface, one has a similar situation. Since the wall acts as a repulsive potential, its

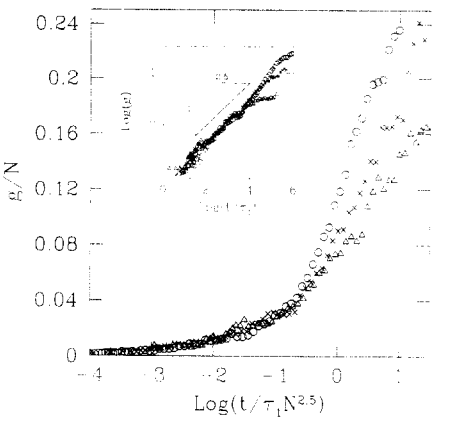

Figure 8. Scaling plot for the attractive case, $\chi = -\ln(2)$. $N = 20$ (triangle), 50 (cross), and 100 (circle). g is scaled by N, and t is scaled by $\tau_1 N^{2.5}$. The inset shows the exponent is indeed close to 0.4.

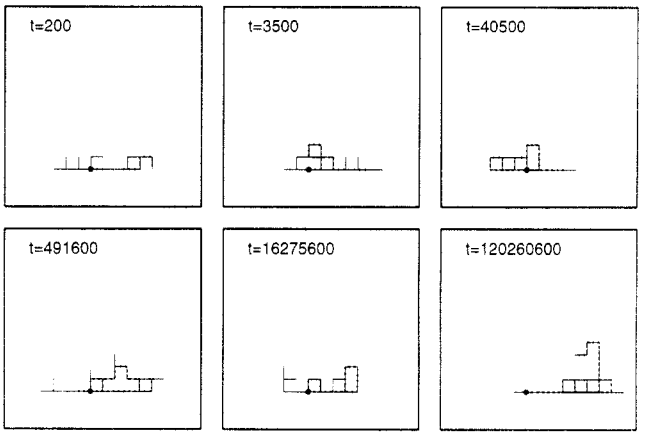

Figure 9. Typical relaxation modes for the attractive case with $\chi = -\ln(2)$. For clarity, the two-dimensional picture is shown here. ($N = 50$). The dotted lines represent primitive paths defined in the text.

removal decreases the effective value of χ, making the interaction attractive when the substrate is not too chemically incompatible with connectors. In this case, one has a large toughness because the grafted chain prefers to stay near the interface region while making "many stitches", of order $N^{1/2}$, between the two rubbers. This situation was recently analyzed by Ji and de Gennes.[4]

Now we discuss the opposite extreme. When the gel swelling is not very significant and the connector chain is compatible with the network, χ is often positive. In addition to the chemical disparity between the chain and the substrate, contamination of the interface can be another reason for the chain to disfavor the surface. In this case, the chain tends to be expelled from the surface more strongly compared to the case $\chi = 0$. Paradoxically, our simulation results suggest that this expulsion slows down the dynamics of chain penetration, although we believe this is an artifact of using Monte Carlo dynamics, as explained below. This is similar to the problem of Monte Carlo dynamics for DNA gel electrophoresis in a strong field, which has been investigated in recent years.[25-27]

Extruded defects driven by the strong surface repulsion grow until the tension becomes large enough to counteract the repulsive force from the wall. The chain at the wall, being under high tension, should be quite taut. The lack of kinks at the wall means that the dynamics become slow in this region. This is unphysical because in reality even a completely taut chain can diffuse, whereas the dynamics used here do not have collective motions allowing a defect-

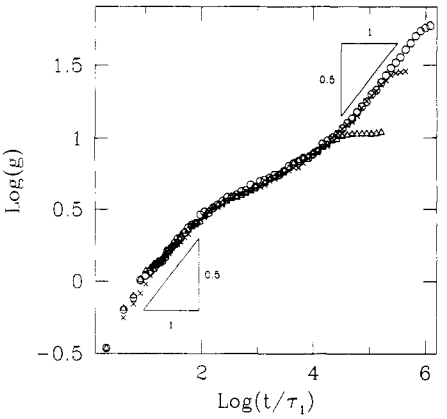

Figure 10. Repulsive case with $\chi = \ln(10)$. $N = 20$ (triangle), 50 (cross), and 100 (circle). The initial growth is close to $t^{1/2}$, but the growth is slowed down gradually. After the Rouse time, it regains momentum and $t^{1/2}$ growth resumes. Finally it crosses over to logarithmic behavior.

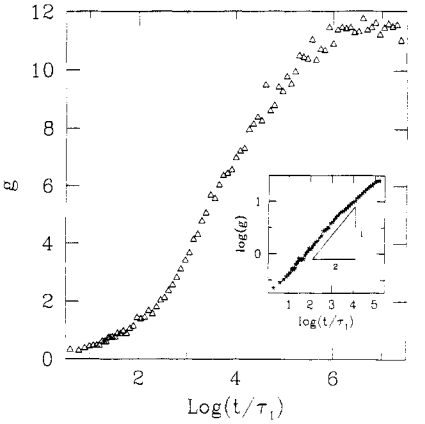

Figure 11. Effect of entanglements in the slab. $d_s = 0$. The graph was obtained with $N = 20$. During the period 10^4–10^6, the growth is logarithmic. The inset with $N = 100$ shows the initial growth has a $t^{1/2}$ dependence.

free segment to move. Another way of seeing the difficulty is that a kink traveling onto the surface must surmount an energy barrier of χ which slows down the dynamics considerably when χ is large. This is an artifact of Monte Carlo simulations with local dynamics.[25] This difficulty can be overcome by either using a Monte Carlo model with long-range moves[26] or using dynamics that are continuous in time.[27] The situation here is not as serious as with electrophoresis where potential energy scales linearly with chain length. The slowing down here is a result of an activation free energy barrier $\propto k_B T\chi$, with no dependence on the size of the defect. Therefore on a sufficiently long time scale the power law behavior should be the same as when $\chi = 0$ and a $t^{1/2}$ growth is observed. This interesting but spurious behavior is shown in Figure 10 for $N = 20$, 50, and 100 with $\chi = \ln(10)$.

5. Interfacial Entanglement Effects

Now we study the effects of putting entanglements in the interface region itself. There are some situations where interfacial entanglements might become important. Suppose for example that the substrate of the tethered chain embedded in a thin layer containing a slightly incompatible polymer network. Before adhesion to the compatible network, the tethered chain is allowed to relax in the embedded layer. This situation is similar to the case of negative χ discussed in section 4.1.2. After some time the chain will become intertwined with this layer of material. Upon attachment of the compatible network it will move into it, but now its motion is more highly constrained due to the presence of entanglements in the thin layer. We will now see that these surface entanglements have a dramatic effect on the dynamics of the grafted chains.

The model studied in section 4 must be modified to take into account this entanglement effect in the interface region. For simplicity, we assume that the entanglement length in this region is the same as in the network. Also in the simulations we are assuming as before that the lattice size of the cage equals the distance between monomers. The tethered chain now moves along a small tube not only in the three-dimensional network but also in the two-dimensional interface region.

Before we consider the relaxation of this entangled chain, it should be noted that the primitive length of the initial conformation is close to its equilibrium value, since it is already constrained to a tube. As one can see from eq 10, the three-dimensional value of the equilibrium primitive length is $2N/3$, whereas the two-dimensional value is $N/2$. This should be compared with the previous situation where the initial primitive length was just the end-to-end distance of a Gaussian chain in a slab which is of order $N^{1/2}$.

Because here the initial value of the primitive length is 25% less than in equilibrium, the chain slightly expands its primitive path while penetrating into the gel. Kinks on the surface feel a repulsive entropic force which causes them to escape by climbing up the free end to avoid the surface. The inset in Figure 11 shows the initial growth of the plume. As the figure shows, the exponent of g as a function of time is 1/2, because this is a diffusive process. This regime lasts until $t \sim \tau_1 N^2$. By the end of this time the primitive length of the chain has increased by of order N monomers.

Viewed at this time scale, the end of the chain has formed a small plume and the rest of the chain is in a tube embedded in the interface. At longer time scales, the dynamics become very slow and similar to the case of no interfacial entanglements. In order for the tube to escape into the gel, the chain has to overcome a free energy barrier as in the previous section. From a relaxation time formula similar to eq 8 or eq 9, we obtain

$$g(t) \approx \frac{d_e}{a}\left[N \ln\left(\frac{t}{\tau_1 N^2}\right)\right]^{1/2} \qquad (11)$$

This spans the major part of the healing process. In other words, only a fraction of the toughness is recovered in a time scale $\tau_1 N^2$, and to recover almost all the toughness takes a time exponential in the chain length. This should be contrasted with the case of no interfacial entanglements. There almost all the toughness is recovered in the time scale $\tau_1 N^2$.

The entire relaxation behavior is shown in Figure 11 for $N = 20$. A crossover to logarithmic behavior after $t \sim 10^3 \tau_1$ is evident in this figure.

Figure 12 is to be compared with Figure 4.

6. Conclusion

We have investigated the healing process of the interface between a cross-linked elastomer and a grafted solid. As the grafted chain penetrates into the network the toughness increases due to entanglements. The dynamics of the grafted polymer was studied by Monte Carlo simulation under various conditions. In the case of $\chi \geq 0$ the general features have been found to be in good agreement with the predictions of O'Connor and McLeish.[6]

As soon as the contact is made, the grafted chain starts to penetrate into the rubber network at a distance of order

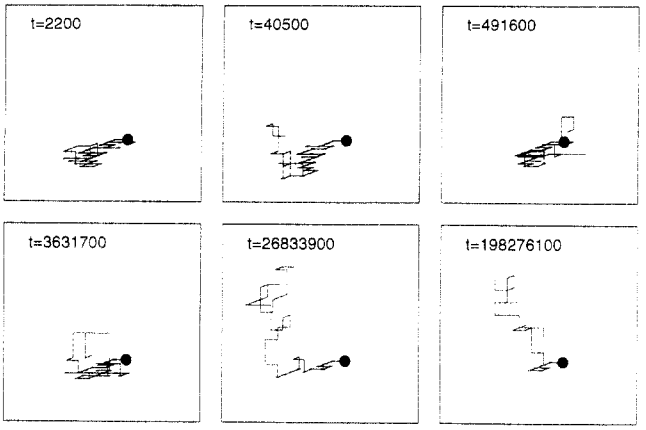

Figure 12. Vertical growth of the chain when there is entanglement in the slab. $N = 50$. The free end starts to penetrate slowly and the growth is logarithmic after the time scale N^2. After 3 $\times$ 10^6 MCS's, an appreciable number of chain segments are still at the interface.

$\sim N^{1/2}a$ from the anchor point. If there is no interaction between the grafted chain and the surface, the primitive length in the penetrated part increases as $t^{1/2}$. This process persists up to a time scale $\tau_1 N^2$. In the case of no interfacial entanglements, almost all the chain segments penetrate into the network in this time scale. After this rapid penetration stage, logarithmic relaxation follows. When attractive interactions between the chain and the substrate were added, the initial dynamics were found to be slower. In the attractive case, the power scaling law is $g(t) \sim t^{2/5}$.

If topological constraints are added in the interface, the relaxation is found to be logarithmic after the time scale $\tau_1 N^2$. The dynamics become similar to the arm of a star polymer, which has logarithmic relaxation. The time to reach full toughness in this case can easily exceed days or weeks in quite reasonable experimental situations using moderate size polymers. We can conclude that toughness recovery is very sensitive to the conditions in the interface. To get the best result for adhesion, we have to eliminate the possibility of entanglements in the surface before attachment.

In this work, the wall did not play a crucial role. One expects qualitatively similar behavior for the adhesion between two different polymer networks. Similar relaxation behavior is expected for a grafted chain. But the interpretation for the toughness recovery should be modified because this is a many-stitch problem as discussed earlier.

The case of tethered polymers at interfaces under shear is more difficult to simulate. The problem of large tensions causes problems with Monte Carlo dynamics as mentioned earlier. These can be overcome by using long-range moves[26] or continuous time dynamics.[27] We are currently investigating both of these techniques.

Acknowledgment. We would like to thank H. R. Brown for suggesting this problem and for several valuable discussions. This work was supported by NSF Grant DMF-9112767.

References and Notes

(1) Raphaël, E.; de Gennes, P.-G. *J. Phys. Chem.* **1992**, *96*, 4002–4007.
(2) de Gennes, P.-G. *J. Phys. Fr.* **1989**, *50*, 2551–2562.
(3) Brown, H. R. *Annu. Rev. Mater. Sci.* **1991**, *21*, 463–489.
(4) Ji, H.; de Gennes, P.-G. *Macromolecules* **1993**, *26*, 520–525.
(5) Evans, K. E. *J. Polym. Sci., Polym. Phys. Ed.* **1987**, *25*, 353–368.
(6) O'Connor, K. P.; McLeish, T. C. B. *Macromolecules* **1993**, *26*, 7322–7325.
(7) Reichert, W. F.; Brown, H. R. *Polymer* **1993**, *34* (11), 2289.
(8) Creton, C.; Brown, H. R.; Shull, K. R. IBM preprint, 1993.
(9) Brown, H. R. *Macromolecules* **1993**, *26* (7), 1666–1670.
(10) Johnson, K. L.; Kendall, K.; Roberts, A. D. *Proc. R. Soc. London, A* **1971**, *324*, 301.
(11) Brown, H. R.; Hui, C.-Y.; Raphaël, E. *Macromolecules* **1994**, *27* (2), 608–609.
(12) Doi, M. *Polym. J.* **1973**, *5*, 288.
(13) Evans, K. E.; Edwards, S. F. *J. Chem. Soc., Faraday Trans. 2* **1981**, *77*, 1891–1912.
(14) Edwards, S. F.; Evans, K. E. *J. Chem. Soc., Faraday Trans. 2* **1981**, *77*, 1913–1927.
(15) Evans, K. E.; Edwards, S. F. *J. Chem. Soc., Faraday Trans. 2* **1981**, *77*, 1929–1938.
(16) de Gennes, P.-G. *J. Chem. Phys.* **1971**, *55* (2), 572–579.
(17) Doi, M.; Edwards, S. F. *The Theory of Polymer Dynamics*; Clarendon Press: Oxford, 1986.
(18) de Gennes, P.-G. *Scaling Concepts in Polymer Physics*; Cornell University Press: Ithaca, NY, 1979.
(19) Cates, M. E.; Deutsch, J. M. *J. Phys. Fr.* **1986**, *47*, 2121–2128.
(20) Khokhlov, A. R.; Nechaev, S. K. *Phys. Lett.* **1985**, *112A* (3,4), 156–160.
(21) de Gennes, P.-G. *J. Phys. Fr.* **1975**, *36* (12), 1199–1203.
(22) Pearson, D. S.; Helfand, E. *Macromlecules* **1984**, *17*, 888–895.
(23) Helfand, E.; Pearson, D. S. *J. Chem. Phys.* **1983**, *79*, 2054–2059.
(24) Mehta, A.; Needs, R. J.; Thouless, D. J. *Europhys. Lett.* **1991**, *14* (2), 113–117.
(25) de la Cruz, M. O.; Deutsch, J. M.; Edwards, S. F. *Phys. Rev. A* **1986**, *33*, 2047–2055.
(26) Deutsch, J. M.; Reger, J. D. *J. Chem. Phys.* **1991**, *95* (3), 2065–2071.
(27) Deutsch, J. M.; Madden, T. L. *J. Chem. Phys.* **1988**, *90* (4), 2476–2485.
(28) The primitive path in the slab is defined in this work by a straight line between the two end points.